Shihua Wang ✉
Shaolin Hu
Qinghua Zhang

https://doi.org/10.21278/TOF.471040722
ISSN 1333-1124
eISSN 1849-1391

THE MATTHEW EFFECT OF A FAULT CLASSIFICATION MECHANISM AND ITS APPLICATION

Summary

When using the classification algorithm to classify a single sample, the classification accuracy often cannot achieve an ideal effect. To solve this problem, the following two aspects of research work are carried out and presented in this paper. On the one hand, according to the memory characteristics of mechanical faults, a voting classification mechanism for the sample sequence to be classified is proposed. It is found that the classification mechanism of the sample sequence to be classified with memory has the Matthew effect of accumulated advantage. Using this effect, one can improve the accuracy of fault classification. On the other hand, because the length of the sample sequence to be classified increases, the delay of the classification results increases. To solve this problem, the classification algorithm is optimized to minimize the delay on the assumption that the classification accuracy meets the expected requirements.

Key words: *fault diagnosis, machine learning, the Matthew effect*

1. Introduction

With the increasing complexity of industrial processes and large-scale production, it is of great significance to identify and diagnose the fault in industrial processes [1]. Since Niederlinski proposed the idea of fault diagnosis and fault tolerance in the 1970s [2], fault diagnosis methods have been classified into three categories: based on knowledge, based on a model, and based on signal processing [3].

The model-based fault diagnosis method was originally developed by Beard in 1971 [4]. In the method, hardware redundancy is replaced by analytical redundancy [4]. In terms of comprehensive result recordings, there are a few studies on model-based fault diagnosis methods [5-8]. Regarding the stability problem of input and output limits, an operator-based fault detection method is proposed in the study [6] to detect the fault of the drive and the input constraint in an aluminium plate heating process. A model-based method for fault diagnosis in controlling systems and robot systems is presented in [7, 8].

The studies [9-11] proposed a model-based sensor approach to determine fault detectability and isolability of a linear time-invariant system based on a parity equation. The approach was applied to examine the fault detectability and isolability of the motor-driven

power steering system. In the study [12], a discrete hidden Markov model fault diagnosis strategy was proposed to solve the fault classification problems. These model-based fault diagnosis methods are suitable for systems that have a sufficient number of sensors and information. The mechanism of the process could be fully exploited to establish an accurate quantitative mathematical model [13,14]. In the study [15], Descartes' three-dimensional coordinate system of fault diagnosis is put forward; it carries out the function of real-time diagnosis of the measurement system.

Knowledge-based fault diagnosis methods are presented in [16-20]. Ding et al. [16] proposed the static key performance index prediction and diagnosis method, which improved the probability of prediction and diagnosis of complex industrial process faults. The method is also applied to fault diagnosis of industrial hot strip mills. In the study [17], a new method based on potential kernel function technology, pseudo-sample speculation, and intermittent process fault identification and diagnosis is proposed; the method deals with the problems of pass and fail in operation. A two-stage approach to fault diagnosis using knowledge is proposed in the study [18]. A novel unsupervised domain adaptation approach that reduces distribution shifts for cross-domain fault detection is presented in [19]. The knowledge-based fault diagnosis method is suitable for systems that do not have a sufficient number of sensors, sufficient information, or an analytical model [20].

Fault diagnosis methods based on data processing are dealt with in [21-28]. Estima and Cardoso [21] proposed a diagnosis method to solve the problem of a motor being prone to serious faults by measuring the motor current phase and its corresponding reference signal. In order to improve the reliability of the sensor and the safety of the whole system in the aircraft control system, Samara et al. [22] proposed a statistical method in which the covariance of the induced signal is applicable to feature extraction. Wen et al.[23] presented a signal-to-image conversion method, and applied the convolution neural network models to the fault diagnosis field. In the study [24] a novel fault detection method, the K-nearest neighbour algorithm (KNN), is proposed to isolate multiple sensor faults under a less strict condition. In the study [25], a novel multi-resolution convolution neural network for biometric human identification is dealt with; the method also effectively handles the blind signal processing. A variant of deep residual networks to improve diagnostic performance is presented in the study [26]. Finally, the studies [27,28] presented a data-driven multi-label pattern identification approach to identify complicated faults rapidly and accurately . Moreover, the proposed approach has the potential to be extended to other diagnosis cases in which the dynamics of multiple variables is involved.

With the increase in the number of process parameters, fault diagnosis data-driven approach is becoming increasingly popular [29]. The fault diagnosis method based on data can perform fault diagnosis by analysing and processing the process monitoring data. The fault diagnosis is implemented without prior knowledge of the system and the accurate model of the system. Since data acquisition is easier than accurate system modelling, the data-driven fault diagnosis method is a more feasible approach [30-31]. Many researchers have studied the data-driven fault diagnosis method, which involves many techniques, such as multivariate statistical analysis [32], neural network [33], evidence theory [34-36], and support vector machine (SVM) [37,38].

Scientists have extensively researched mechanical fault diagnosis [15,28,29,39,40], but no relevant research on the memory characteristics of mechanical fault diagnosis has been carried out. In this paper, we first study the memory characteristics of mechanical faults, and then propose a fault classification model based on the memory characteristics of mechanical faults. In this model, the diagnosis delay is minimized on the basis of ensuring the accuracy of fault diagnosis.

2. Definitions and Properties of the Sample Sequence with Memorability

2.1 Definitions of the Sample Sequence with Memorability

As shown in Fig. 1, class 1 indicates a normal state and class 2 indicates a fault state. The gear-tooth-missing fault is taken as an example; if the gear-tooth-missing fault occurs at the (k_1+1)th time point, the mechanical equipment cannot fix itself. Therefore, the running state of the mechanical equipment was kept in the fault state until the gear-tooth-missing fault was repaired at the (k_2+1)th time point. That is, all samples from $sample_{k_1+1}$ to $sample_{k_2}$ belong to class 2. Similarly, all samples from $sample_{k_2+1}$ to $sample_{k_3}$ belong to class 1.

Set $\{sample_1, sample_2, \cdots, sample_n, \cdots\}$ represents a set of consecutive samples of the running mechanical equipment to be measured. If the running mechanical equipment state has not changed, all samples of the set $\{sample_1, sample_2, \cdots, sample_n, \cdots\}$ are of the same category. The sample sequence with memorability is defined as follows.

Definition 1 Formula (1), $S_m (m = 1, 2, \cdots)$ is called the sample sequence with memorability, and set L_m is called the memorability length of S_m.

$$S_1 = \{sample_1, \cdots, sample_{L_1}\}, \quad \cdots, \quad S_m = \{sample_m, \cdots, sample_{m+L_m-1}\}, \quad \cdots \tag{1}$$

As shown in Formula (2), the sample in the set S_m is a time series. We need to focus on the first sample, $sample_m$, and the sequence length L_m.

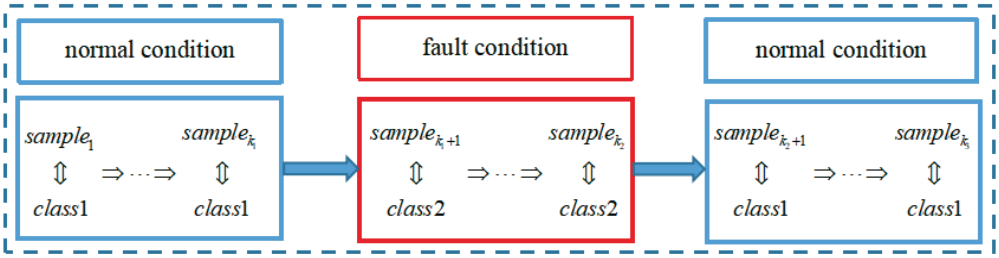

Fig. 1 Schematic diagram of memory characteristics of equipment running state

2.2 Confusion Matrix of Fault Classification

Table 1 shows the confusion matrix of binary classification problems, and Table 2 shows the confusion matrix of multi-classification problems.

Table 1 Confusion matrix of binary classification

Confusion matrix		**Classification**	
		positive	negative
Condition	positive	true positive	false positive
	negative	false negative	true negative

$$Accuracy = \frac{true\ positive + true\ negative}{true\ positive + false\ positive + true\ negative + false\ negative} \tag{2}$$

For the convenience of the following description, Formula (2) is given on the basis of Formula (1).

$$P_{11}=\frac{true\ positive}{true\ positive+false\ positive} \qquad P_{12}=\frac{false\ positive}{true\ positive+false\ positive}$$

$$P_{21}=\frac{false\ negative}{true\ negative+false\ negative} \qquad P_{22}=\frac{true\ negative}{true\ negative+false\ negative} \tag{3}$$

For the multi-classification problem, the calculation formula of P_{ij} is given with reference to Formula (3), as shown in Formula (4); $P_{ij}(i=1,\ 2;\ j=1,\ 2)$ indicates the proportion of the test samples, where *i* is the actual label and *j* is the predicted label. Table 3 shows the prediction accuracy of each class.

$$P_{ij}=\frac{Num_{ij}}{\sum_{k=1}^{n}Num_{ik}},\ (i=1,\ 2,\ \cdots,\ n) \tag{4}$$

Table 2 Confusion matrix of multi-classification

	Predict label 1	**Predict label 2**	**... ...**	**Predict label *n***
Class 1	Num_{11}	Num_{12}	... ...	Num_{1n}
Class 2	Num_{21}	Num_{22}	... ...	Num_{2n}
... ...	... ...	... ...	... ...	... ...
Class n	Num_{n1}	Num_{n2}	... ...	Num_{nn}

Table 3 Prediction accuracy of each class

	Predict label 1	**Predict label 2**	**... ...**	**Predict label n**
Class 1	P_{11}	P_{12}	... ...	P_{1n}
Class 2	P_{21}	P_{22}	... ...	P_{2n}
... ...	... ...	... ...	... ...	... ...
Class n	P_{n1}	P_{n2}	... ...	P_{nn}

2.3 Prediction Accuracy of the Sample Sequence with Memorability

For the multi-classification problems of fault diagnosis, the prediction label, and the prediction accuracy of the sample sequence S_m are defined as follows.

Definition 2 If the number of samples labelled as k is greater than the number of the samples that have other labels in $S^{[L]}$ (the Lth sample sequence), then $S^{[L]}$ is labelled as k.

Definition 2 represents the voting mechanism of the prediction label of the sample sequence.

$$P_{ik}^{[L]}\ (k=1,\ 2;\ i=1,\ 2;\ L\in N^{+}) \tag{5}$$

Assuming that the actual class label for all samples is *i*, Formula (5) indicates the probability that the prediction label of the sample sequence is *k*.

When computing $P_{ik}^{[L]}$, a definition is needed. Moreover, when computing the prediction label of the sample sequence S_m, it is possible that the number of samples of two or more prediction labels is the maximum. Consequently, definition 2 needs to be advanced.

Definition 3 For binary classification problem, if the number of samples with prediction label 1 and label 2 in the sample sequence is equal, the probability of the sample sequences that are predicted to be label 1 and label 2 is 1/2. For the multi classification problem, if the frequencies of Q prediction labels are the largest, the probability of the sample sequence that is predicted as any of these Q labels is 1/Q.

2.4 Theorem and Properties of the Sample Sequence with Memorability

For binary classification problems, the prediction accuracy $P_{ik}^{[L]}$ of sample sequences S_m has the following properties and theorems.

Property 1 Let $\tilde{P}_{ii}^{[2m-1]}=\sum_{k=m}^{2m-1}\binom{2m-1}{i}P_{ii}^{k}(1-P_{ii})^{2m-1-k}$, $\tilde{P}_{ii}^{[2m]}=\sum_{k=m+1}^{2m}\binom{2m}{k}P_{ii}^{k}(1-P_{ii})^{2m-k}$,

$\tilde{P}_{ii}^{[2m+1]}=\sum_{m+1}^{2m+1}\binom{2m+1}{k}P_{ii}^{k}(1-P_{ii})^{2m+1-k}$, then

$$\tilde{P}_{ii}^{[2m]}-\tilde{P}_{ii}^{[2m-1]}=-\binom{2m-1}{m}P_{ii}^{m}(1-P_{ii})^{m},\ \tilde{P}_{ii}^{[2m+1]}-\tilde{P}_{ii}^{[2m]}=\binom{2m}{m}P_{ii}^{m+1}(1-P_{ii})^{m}.$$

Proof: According to the Pascal triangle formula, we have

$$\begin{aligned}&\binom{2m}{2m}P_{ii}^{2m}+\binom{2m}{2m-1}P_{ii}^{2m-1}(1-P_{ii})-\binom{2m-1}{2m-1}P_{ii}^{2m-1}=\binom{2m}{2m-1}P_{ii}^{2m-1}(1-P_{ii})-\binom{2m-1}{2m-1}P_{ii}^{2m-1}(1-P_{ii})\\&=\binom{2m-1}{2m-2}P_{ii}^{2m-1}(1-P_{ii})\end{aligned}$$

$$\begin{aligned}&\binom{2m}{2m}P_{ii}^{2m}+\binom{2m}{2m-1}P_{ii}^{2m-1}(1-P_{ii})-\binom{2m-1}{2m-1}P_{ii}^{2m-1}-\binom{2m-1}{2m-2}P_{ii}^{2m-2}(1-P_{ii})\\&=\binom{2m-1}{2m-2}P_{ii}^{2m-1}(1-P_{ii})-\binom{2m-1}{2m-2}P_{ii}^{2m-2}(1-P_{ii})\\&=-\binom{2m-1}{2m-2}P_{ii}^{2m-2}(1-P_{ii})^{2}\end{aligned}$$

$$\tilde{P}_{ii}^{[2m]}-\tilde{P}_{ii}^{[2m-1]}=\sum_{k=m+1}^{2m}\binom{2m}{k}P_{ii}^{k}(1-P_{ii})^{2m-k}-\sum_{k=m}^{2m-1}\binom{2m-1}{i}P_{ii}^{k}(1-P_{ii})^{2m-1-k}=-\binom{2m-1}{m}P_{ii}^{m}(1-P_{ii})^{m}$$

$$\begin{aligned}\tilde{P}_{ii}^{[2m+1]}-\tilde{P}_{ii}^{[2m]}&=\sum_{m+1}^{2m+1}\binom{2m+1}{k}P_{ii}^{k}(1-P_{ii})^{2m+1-k}-\sum_{k=m+1}^{2m}\binom{2m}{k}P_{ii}^{k}(1-P_{ii})^{2m-k}\\&=-\binom{2m}{m+1}P_{ii}^{m+1}(1-P_{ii})^{m}+\binom{2m+1}{m+1}P_{ii}^{m+1}(1-P_{ii})^{m}=\binom{2m}{m}P_{ii}^{m+1}(1-P_{ii})^{m}\end{aligned}$$

Property 2 For the binary classification problems of fault diagnosis, the prediction accuracy of the sample sequence with memorability satisfies

$$P_{ik}^{[2m]} = P_{ik}^{[2m-1]},\ (i=1,\ 2;\ k=1,\ 2;\ m \in N^{+}).$$

Proof: Without loss of generality, we show that when i=1, k=1, we have $p_{11}^{[2m]} = p_{11}^{[2m-1]}$.

$$\because \binom{2m}{2m} = \binom{2m-1}{2m-1} = 1,\ \therefore\ \binom{2m}{2m} P_{ii}^{2m} - \binom{2m-1}{2m-1} P_{ii}^{2m-1} = -\binom{2m-1}{2m-1} P_{ii}^{2m-1}(1-P_{ii})$$

Known from property 1, $\tilde{P}_{11}^{[2m]} - \tilde{P}_{11}^{[2m-1]} = -\binom{2m-1}{m} P_{11}^{m}(1-P_{11})^{m}$

$$\therefore P_{11}^{[2m]} - P_{11}^{[2m-1]} = \frac{1}{2}\binom{2m}{m} P_{11}^{m} P_{12}^{m} - \binom{2m-1}{m} P_{11}^{m} P_{12}^{m} = 0,\ \therefore P_{11}^{[2m]} = P_{11}^{[2m-1]}.$$

Some properties and theorems about binary classification and three classification problems are given below.

Theorem 1 For the binary classification problems of fault diagnosis, if $P_{ik} > \frac{1}{2}$ ($P_{ik} < \frac{1}{2}$), (i=1, 2; j=1, 2), then sequence $\left\{P_{ik}^{[2m-1]}\right\}$ is monotonically increasing (decreasing).

Proof: Without loss of generality, we show when i=1, k=1, $P_{11}^{[2m+1]} > P_{11}^{[2m-1]}$.

Known from property 1, $\tilde{P}_{11}^{[2m+1]} - \tilde{P}_{11}^{[2m]} = \binom{2m}{m} P_{11}^{m+1}(1-P_{11})^{m}$,

$$\because\ P_{11} + P_{12} = 1,\ \therefore\ P^{[2m+1]} - P^{[2m]} = \binom{2m}{m} P_{11}^{m+1} P_{12}^{m} - \frac{1}{2}\binom{2m}{m} P_{11}^{m} P_{12}^{m} = (P_{11} - \frac{1}{2})\binom{2m}{m} P_{11}^{m} P_{12}^{m}$$

$$\because P_{11} > \frac{1}{2},\quad \therefore P_{11}^{[2m+1]} > P_{11}^{[2m]}.$$

$$\because P_{11}^{[2m]} = P_{11}^{[2m-1]}, \therefore P_{11}^{[2m+1]} > P_{11}^{[2m-1]}.$$

Consequently, $\left\{P_{ii}^{2m-1}\right\}$ is monotonically increasing.

Corollary 1 For the binary classification problems of fault diagnosis, if $P_{ik} > \frac{1}{2}$ ($P_{ik} < \frac{1}{2}$), (i=1, 2; j=1, 2), then sequence $\left\{P_{ik}^{[2m]}\right\}$ is monotonically increasing (decreasing);

Corollary 2 For the binary classification problems of fault diagnosis, if $P_{ik} > \frac{1}{2}$ ($P_{ik} > \frac{1}{2}$), (i=1, 2; j=1, 2), then $P_{ii}^{[n+1]} \geq P_{ii}^{[n]}$ ($P_{ii}^{[n+1]} \leq P_{ii}^{[n]}$);

Property 3 $P_{ij}^{[2]} = P_{ij}^{[1]}$

Proof: $\because P_{ij}^{[1]} = \binom{1}{1} P_{ij} = P_{ij},\ P_{ij}^{[2]} = \binom{2}{2} P_{ij}^{2} + \frac{1}{2}\binom{2}{1} P_{ij} \sum_{k \neq j} P_{ik} = P_{ij} \sum_{k=1}^{n} P_{ik} = P_{ij},\ \therefore P_{ij}^{[2]} = P_{ij}^{[1]}$

Theorem 2 For the three classification models, if $P_{ii} > P_{ik}$, $(k \neq i)$, then $P_{ii}^{[m+1]} > P_{ii}^{[m]}$, $(m \geq 2)$.

Proof: Without loss of generality, we show when i=1, k=1, $P_{11}^{[m+1]} > P_{11}^{[m]}$. Firstly, $P_{11}^{[6]} > P_{11}^{[5]} > P_{11}^{[4]} > P_{11}^{[3]} > P_{11}^{[2]}$ is proved to be true. Known from definition 2,

$$P_{11}^{[2]} = \binom{2}{2} P_{11}^2 + \frac{1}{2}\binom{2}{1} P_{11}(P_{12} + P_{13})$$

$$P_{11}^{[3]} = \sum_{k=2}^{3} \binom{3}{k} P_{11}^k (P_{12} + P_{13})^{3-k} + \frac{1}{3}\binom{3}{1}\binom{2}{1} P_{11} P_{12} P_{13}$$

$$P_{11}^{[4]} = \sum_{k=3}^{4} \binom{4}{k} P_{11}^k (P_{12} + P_{13})^{4-k} + \binom{4}{2} P_{11}^2 \left[\frac{1}{2}\binom{2}{2} P_{12}^2 + \binom{2}{1} P_{12} P_{13} + \frac{1}{2}\binom{2}{0} P_{13}^2 \right]$$

$$P_{11}^{[5]} = \sum_{k=3}^{5} \binom{5}{k} P_{11}^k (P_{12} + P_{13})^{5-k} + \binom{5}{2} P_{11}^2 \left[\frac{1}{2}\binom{3}{2} P_{12}^2 P_{13} + \frac{1}{2}\binom{3}{1} P_{12} P_{13}^2 \right]$$

$$P_{11}^{[6]} = \sum_{k=4}^{6} \binom{6}{k} P_{11}^k (P_{12} + P_{13})^{6-k} + \binom{6}{3} P_{11}^3 \left[\frac{1}{2}\binom{3}{3} P_{12}^3 + \sum_{j=1}^{2} \binom{3}{j} P_{12}^j P_{13}^{3-j} + \frac{1}{2}\binom{3}{0} P_{13}^3 \right] + \frac{1}{3}\binom{6}{2}\binom{4}{2} P_{11}^2 P_{12}^2 P_{13}^2$$

Known from property 2, $\tilde{P}_{11}^{[3]} - \tilde{P}_{11}^{[2]} = \binom{2}{1} p_{11}^2 (p_{12} + p_{13})$,

$$\because P_{11} + P_{12} + P_{13} = 1$$

$$\therefore P_{11}^{[3]} - P_{11}^{[2]} = \binom{2}{1} P_{11}^2 (P_{12} + P_{13}) + \frac{1}{3}\binom{3}{1}\binom{2}{1} P_{11} P_{12} P_{13} - \frac{1}{2}\binom{2}{1} P_{11}(P_{12} + P_{13})(P_{11} + P_{12} + P_{13})$$

$$= \left[\binom{2}{1} - \frac{1}{2}\binom{2}{1} \right] P_{11}^2 (P_{12} + P_{13}) + \left[\frac{1}{3}\binom{3}{1}\binom{2}{1} - 2 \cdot \frac{1}{2}\binom{2}{1} \right] P_{11} P_{12} P_{13} - \frac{1}{2}\binom{2}{1} P_{11} P_{12}^2 - \frac{1}{2}\binom{2}{1} P_{11} P_{13}^2$$

$$= \frac{1}{2}\binom{2}{1} P_{11} P_{12}(P_{11} - P_{12}) + \frac{1}{2}\binom{2}{1} P_{11} P_{13}(P_{11} - P_{13}) > 0$$

$$\therefore P_{11}^{[3]} > P_{11}^{[2]}$$

Known from property 2, $\tilde{P}_{11}^{[4]} - \tilde{P}_{11}^{[3]} = -\binom{3}{2} P_{11}^2 (P_{12} + P_{13})^2$,

$$\because P_{11}^{[4]} - P_{11}^{[3]} = \binom{4}{2} P_{11}^2 \left[\frac{1}{2}\binom{2}{2} P_{12}^2 + \binom{2}{1} P_{12} P_{13} + \frac{1}{2}\binom{2}{0} P_{13}^2 \right] - \binom{3}{2} P_{11}^2 (P_{12} + P_{13})^2$$

$$- \frac{1}{3}\binom{3}{1}\binom{2}{1} p_{11} p_{12} p_{13} (p_{11} + p_{12} + p_{13})$$

$$= \frac{1}{3}\binom{3}{1}\binom{2}{1} P_{11} P_{12} P_{13}(P_{11} - P_{12}) + \frac{1}{3}\binom{3}{1}\binom{2}{1} P_{11} P_{12} P_{13}(P_{11} - P_{13}) > 0$$

$$\therefore P_{11}^{[4]} > P_{11}^{[3]}$$

Known from property 2, $\tilde{P}_{11}^{[5]} - \tilde{P}_{11}^{[4]} = \binom{4}{2} P_{11}^3 (P_{12} + P_{13})^2$,

$$\because\ P_{11}^{[5]}-P_{11}^{[4]}=\binom{4}{2}P_{11}^{3}(P_{12}+P_{13})^{2}+\binom{5}{2}P_{11}^{2}\left[\frac{1}{2}\binom{3}{2}P_{12}^{2}p_{13}+\frac{1}{2}\binom{3}{1}P_{12}P_{13}^{2}\right]$$
$$-\binom{4}{2}P_{11}^{2}[\frac{1}{2}\binom{2}{2}P_{12}^{2}+\binom{2}{1}P_{12}P_{13}+\frac{1}{2}\binom{2}{0}P_{13}^{2})](P_{11}+P_{12}+P_{13})$$
$$=\frac{1}{2}\binom{4}{2}\binom{2}{2}P_{11}^{2}P_{12}^{2}(P_{11}-P_{12})+\frac{1}{2}\binom{4}{2}\binom{2}{2}P_{11}^{2}P_{13}^{2}(P_{11}-P_{13})>0$$

$\therefore P_{11}^{[5]}>P_{11}^{[4]}$

Known from property 2, $\tilde{P}_{11}^{[6]}-\tilde{P}_{11}^{[5]}=-\binom{5}{3}p_{11}^{3}(p_{12}+p_{13})^{3}$,

$$\because\ P_{11}^{[6]}-P_{11}^{[5]}=\binom{6}{3}P_{11}^{3}\left[\frac{1}{2}\binom{3}{3}P_{12}^{3}+\binom{3}{2}P_{12}^{2}P_{13}+\binom{3}{1}P_{12}P_{13}^{2}+\frac{1}{2}\binom{3}{0}P_{13}^{3})\right]+\frac{1}{3}\binom{6}{2}\binom{4}{2}P_{11}^{2}P_{12}^{2}P_{13}^{2}$$
$$-\binom{5}{3}P_{11}^{3}(P_{12}+P_{13})^{3}-\binom{5}{2}P_{11}^{2}\left[\frac{1}{2}\binom{3}{2}P_{12}^{2}P_{13}+\frac{1}{2}\binom{3}{1}P_{12}P_{13}^{2})\right](P_{11}+P_{12}+P_{13})$$
$$=\frac{1}{2}\binom{5}{2}\binom{3}{2}P_{11}^{2}P_{12}^{2}P_{13}(P_{11}-P_{12})+\frac{1}{2}\binom{5}{2}\binom{3}{1}P_{11}^{2}P_{12}P_{13}^{2}(P_{11}-P_{13})>0$$

$\therefore P_{11}^{[6]}>P_{11}^{[5]}$

$\therefore P_{11}^{[6]}>P_{11}^{[5]}>P_{11}^{[4]}>P_{11}^{[3]}>P_{11}^{[2]}$.

Next, $P_{11}^{[6m+6]}>P_{11}^{[6m+5]}>P_{11}^{[6m+4]}>P_{11}^{[6m+3]}>P_{11}^{[6m+2]}>P_{11}^{[6m+1]}>P_{11}^{[6m]},(m\in N^{+})$ is proved to be true. Known from definition 2,

$$P_{11}^{[6m]}=\sum_{k=3m+1}^{6m}\binom{6m}{k}P_{11}^{k}(P_{12}+P_{13})^{6m-k}+\frac{1}{3}\binom{6m}{2m}P_{11}^{2m}C_{4m}^{2m}P_{12}^{2m}P_{13}^{2m}+\sum_{j=2m+1}^{3m}\binom{6m}{j}P_{11}^{j}\cdot$$
$$\left[\frac{1}{2}\binom{6m-j}{j}P_{12}^{j}P_{13}^{6m-2j}+\sum_{k=6m-2j+1}^{j-1}\binom{6m-j}{k}P_{11}^{k}(P_{12}+P_{13})^{6m-j-k}+\frac{1}{2}\binom{6m-j}{6m-2j}P_{12}^{6m-2j}P_{13}^{j}\right]$$

$$P_{11}^{[6m+1]}=\sum_{k=3m+1}^{6m+1}\binom{6m+1}{k}P_{11}^{k}(P_{12}+P_{13})^{6m+1-k}+\sum_{j=2m+1}^{3m}\binom{6m+1}{j}P_{11}^{j}\cdot$$
$$\left[\frac{1}{2}\binom{6m+1-j}{j}P_{12}^{j}P_{13}^{6m+1-2j}+\sum_{k=6m+2-2j}^{j-1}\binom{6m+1-j}{k}P_{12}^{k}P_{13}^{6m+1-j-k}+\frac{1}{2}\binom{6m+1-j}{6m+1-2j}P_{12}^{6m+1-2j}P_{13}^{j}\right]$$

$$P_{11}^{[6m+2]}=\sum_{k=3m+2}^{6m+2}\binom{6m+2}{k}P_{11}^{k}(P_{12}+P_{13})^{6m+2-k}+\sum_{j=2m+1}^{3m+1}\binom{6m+2}{j}P_{11}^{j}\cdot$$
$$\left[\frac{1}{2}\binom{6m+2-j}{j}P_{12}^{j}P_{13}^{6m+2-2j}+\sum_{k=6m+3-2j}^{j-1}\binom{6m+2-j}{k}P_{12}^{k}P_{13}^{6m+2-j-k}+\frac{1}{2}\binom{6m+2-j}{6m+2-2j}P_{12}^{6m+2-2j}P_{13}^{j}\right]$$

$$P_{11}^{[6m+3]}=\sum_{k=3m+2}^{6m+3}\binom{6m+3}{k}P_{11}^{k}(P_{12}+P_{13})^{6m+3-k}+\frac{1}{3}\binom{6m+3}{2m+1}P_{11}^{2m+1}\binom{4m+2}{2m+1}P_{12}^{2m+1}P_{13}^{2m+1}+\sum_{j=2m+2}^{3m+1}\binom{6m+3}{j}\cdot$$
$$P_{11}^{j}\left[\frac{1}{2}\binom{6m+3-j}{j}P_{12}^{j}P_{13}^{6m+3-2j}+\sum_{k=6m+4-2j}^{j-1}\binom{6m+3-j}{k}P_{12}^{k}P_{13}^{6m+3-j-k}+\frac{1}{2}\binom{6m+3-j}{6m+3-2j}P_{12}^{6m+3-2j}P_{13}^{j}\right]$$

$$P_{11}^{[6m+4]}=\sum_{k=3m+3}^{6m+4}\binom{6m+4}{k}P_{11}^{k}(P_{12}+P_{13})^{6m+4-k}+\sum_{j=2m+2}^{3m+2}\binom{6m+4}{j}P_{11}^{j}\cdot$$

$$\left[\frac{1}{2}\binom{6m+4-j}{j}P_{12}^{j}P_{13}^{6m+4-2j}+\sum_{k=6m+5-2j}^{j-1}\binom{6m+4-j}{k}P_{12}^{k}P_{13}^{6m+4-j-k}+\frac{1}{2}\binom{6m+4-j}{6m+4-2j}P_{12}^{6m+4-2j}P_{13}^{j}\right]$$

$$P_{11}^{[6m+5]}=\sum_{k=3m+3}^{6m+5}\binom{6m+5}{k}P_{11}^{k}(P_{12}+P_{13})^{6m+5-k}+\sum_{j=2m+2}^{3m+2}\binom{6m+5}{j}P_{11}^{j}\cdot$$

$$\left[\frac{1}{2}\binom{6m+5-j}{j}P_{12}^{j}P_{13}^{6m+5-2j}+\sum_{k=6m+6-2j}^{j-1}\binom{6m+5-j}{k}P_{12}^{k}P_{13}^{6m+5-j-k}+\frac{1}{2}\binom{6m+5-j}{6m+5-2j}P_{12}^{6m+5-2j}P_{13}^{j}\right]$$

$$P_{11}^{[6m+6]}=\sum_{k=3m+4}^{6m+6}\binom{6m+6}{k}P_{11}^{k}(P_{12}+P_{13})^{6m+6-k}+\frac{1}{3}\binom{6m+6}{2m+2}P_{11}^{2m+2}\binom{4m+4}{2m+2}P_{12}^{2m+2}P_{13}^{2m+2}+\sum_{j=2m+3}^{3m+3}\binom{6m+6}{j}\cdot$$

$$P_{11}^{j}\left[\frac{1}{2}\binom{6m+6-j}{j}P_{12}^{j}P_{13}^{6m+6-2j}+\sum_{k=6m+7-2j}^{j-1}\binom{6m+6-j}{k}P_{12}^{k}P_{13}^{6m+6-j-k}+\frac{1}{2}\binom{6m+6-j}{6m+6-2j}P_{12}^{6m+6-2j}P_{13}^{j}\right]$$

Known from property 2, $\tilde{P}_{11}^{[6m+1]}-\tilde{P}_{11}^{[6m]}=\binom{6m}{3m}P_{11}^{3m+1}(P_{12}+P_{13})^{3m}$,

$$P_{11}^{[6m+2]}-P_{11}^{[6m+1]}=\frac{1}{2}\sum_{k=2m+1}^{3m}\binom{6m+1}{k}\binom{6m+1-k}{k}P_{11}^{k}P_{12}^{k}P_{13}^{6m+1-2k}(P_{11}-P_{12})$$

$$+\frac{1}{2}\sum_{k=2m+1}^{3m}\binom{6m+1}{k}\binom{6m+1-k}{6m+1-2k}P_{11}^{k}P_{12}^{6m+1-2k}P_{13}^{k}(P_{11}-P_{12})>0$$

$$P_{11}^{[6m+3]}-P_{11}^{[6m+2]}=\frac{1}{2}\sum_{k=2m+1}^{3m+1}\binom{6m+2}{k}\binom{6m+2-k}{k}P_{11}^{k}P_{12}^{k}P_{13}^{6m+2-2k}(P_{11}-P_{12})$$

$$+\frac{1}{2}\sum_{k=2m+1}^{3m+1}\binom{6m+2}{k}\binom{6m+2-k}{6m+2-2k}P_{11}^{k}P_{12}^{6m+2-2k}P_{13}^{k}(P_{11}-P_{12})>0$$

$$P_{11}^{[6m+4]}-P_{11}^{[6m+3]}=\frac{1}{2}\sum_{k=2m+2}^{3m+1}\binom{6m+3}{k}\binom{6m+3-k}{k}P_{11}^{k}P_{12}^{k}P_{13}^{6m+3-2k}(P_{11}-P_{12})$$

$$+\frac{1}{2}\sum_{k=2m+2}^{3m+1}\binom{6m+3}{k}\binom{6m+3-k}{6m+3-2k}P_{11}^{k}P_{12}^{6m+3-2k}P_{13}^{k}(P_{11}-P_{12})+\frac{1}{3}\binom{6m+3}{2m+1}\binom{4m+2}{2m+1}\cdot$$

$$+P_{11}^{2m+1}P_{12}^{2m+1}P_{13}^{2m+1}(P_{11}-P_{12})+\frac{1}{3}\binom{6m+3}{2m+1}\binom{4m+2}{2m+1}P_{11}^{2m+1}P_{12}^{2m+1}P_{13}^{2m+1}(P_{11}-P_{13})>0$$

$$P_{11}^{[6m+5]}-P_{11}^{[6m+4]}=\frac{1}{2}\sum_{k=2m+2}^{3m+2}\binom{6m+4}{k}\binom{6m+4-k}{k}P_{11}^{k}P_{12}^{k}P_{13}^{6m+4-2k}(P_{11}-P_{12})$$

$$+\frac{1}{2}\sum_{k=2m+2}^{3m+2}\binom{6m+4}{k}\binom{6m+4-k}{6m+4-2k}P_{11}^{k}P_{12}^{6m+4-2k}P_{13}^{k}(P_{11}-P_{12})>0$$

$$P_{11}^{[6m+6]}-P_{11}^{[6m+5]}=\frac{1}{2}\sum_{k=2m+2}^{3m+2}\binom{6m+5}{k}\binom{6m+5-k}{k}P_{11}^{k}P_{12}^{k}P_{13}^{6m+5-2k}(P_{11}-P_{12})$$

$$+\frac{1}{2}\sum_{k=2m+2}^{3m+2}\binom{6m+5}{k}\binom{6m+5-k}{6m+5-2k}P_{11}^{k}P_{12}^{6m+5-2k}P_{13}^{k}(P_{11}-P_{12})>0$$

Theorem 2 is proved.

2.5 Example

Based on the theorems given above, two numerical examples of binary classification problems and multi-classification problems are given respectively.

Example 1 In the binary classification problem of mechanical fault diagnosis, the relationship between the prediction accuracy of memory sequence and the memory length is analysed in four cases: case 1 is P_{11}=0.55, case 2 is P_{11}=0.65, case 3 is P_{11}=0.75, and case 4 is P_{11}=0.85.

Table 4 Prediction accuracy of each class

	P_{11}=0.55	P_{11}=0.65	P_{11}=0.75	P_{11}=0.85
***L*=10**	0.621	0.828	0.951	0.994
***L*=20**	0.671	0.913	0.991	1.000
***L*=30**	0.707	0.952	0.998	1.000
***L*=40**	0.736	0.973	1.000	1.000
***L*=50**	0.760	0.985	1.000	1.000

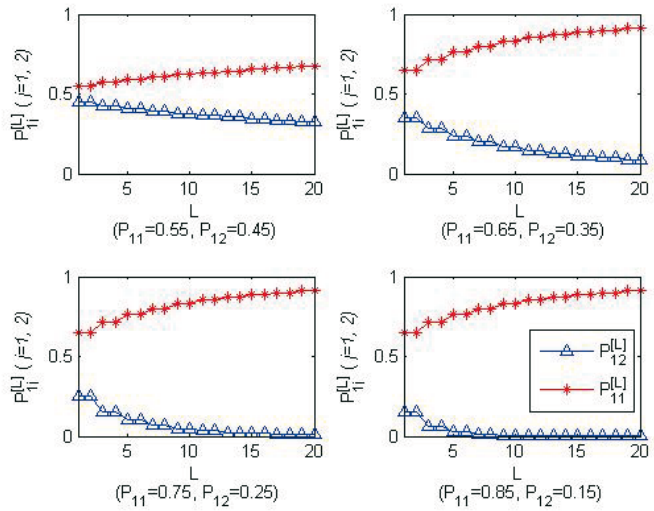

Fig. 2 Correct probability of the sequence with the sequence length

Table 5 Correct probability of the sequence with the sequence length

	P_{11}=0.40	P_{12}=0.35	P_{13}=0.25
***L*=10**	0.843	0.151	0.006
***L*=20**	0.927	0.072	0.001
***L*=30**	0.962	0.038	0
***L*=40**	0.980	0.020	0
***L*=50**	0.989	0.019	0
***L*=60**	0.994	0.006	0

In Fig. 2 and Table 4, the variations of the prediction accuracy of the sample sequence with the memory length are given when P_{11} are 0.55, 0.65, 0.75, and 0.85, respectively. The prediction accuracy of the sample sequence increases gradually with the increase in sequence length. Taking case 1 as an example, since $P_{11} > P_{12}$ satisfies the condition of Theorem 1, it

can be seen from Figure 2 that $P_{11}^{[L]}$ increases with the increase in L and $P_{12}^{[L]}$ decreases with the increase in L. The conclusion of the other three cases is the same as that of case 1. Moreover, it can be seen that when the value of P_{11} is large, the growth rate of $P_{11}^{[L]}$ is faster.

Example 2 In the multi-classification problem of mechanical fault diagnosis, the relationship between the prediction accuracy of memory sequence and the memory length is analysed in four cases: case 1 is P_{11}=0.40, P_{12}=0.35, P_{13}=0.25, case 2 is P_{11}=0.50, P_{12}=0.30, P_{13}=0.20, case 3 is P_{11}=0.60, P_{12}=0.30, P_{13}=0.10, and case 4 is P_{11}=0.70, P_{12}=0.20, P_{13}=0.10.

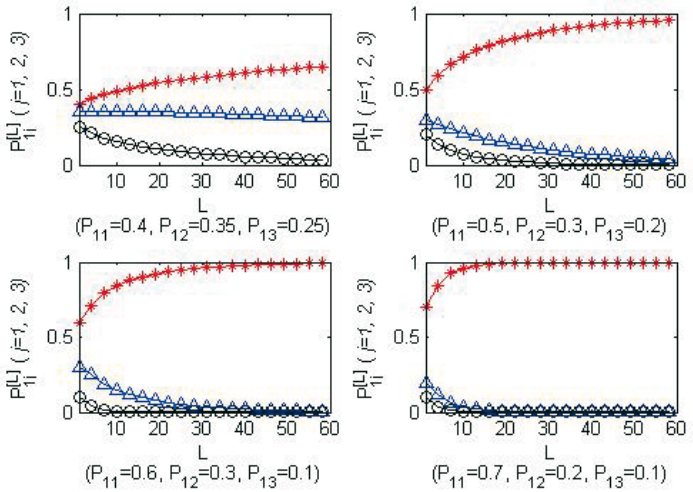

Fig. 3 Correct probability of the sequence with the sequence length

It can be seen from Fig. 3 and Table 5 that examples 2 and 1 have the same conclusion.

3. Minimum delay model under accuracy constraint

According to the theory in Section 2, on the one hand, the increase in diagnostic sample sequence length can improve the prediction accuracy; on the other hand, the increase in diagnostic sample sequence length increases the delay in diagnostic results. To solve this problem, the design of a diagnosis delay minimization model, on the assumption that the accuracy of fault diagnosis is ensured, is discussed below.

Step 1: select an appropriate classification algorithm to make the classification accuracy meet the conditions of theorem 2, that is $P_{ii} > P_{ik}$, $(k \neq i)$.

Step 2: according to the model (6), use the classification algorithm to obtain the prediction accuracy of each fault type, as shown in Table 1, and calculate $L_i (i = 1, 2, \cdots, n)$ according to the prediction accuracy.

$$\begin{aligned} &\min\ L_i \\ &s.t.\quad P_{ii}^{[L_i]} \geq b_i \end{aligned} \tag{6}$$

Step 3: For vector $(i_s, L_{i_s}, i_{s'})$, use i_S that represents the sample prediction label at time s, and use $i_{s'}$ that represents the prediction label of the sample sequence with length L_i. If i_S and $i_{s'}$ are consistent, the prediction label at time s is i_S.

4. Experimental Results

4.1 Experiment Purpose

The first purpose is to evaluate whether the test set reconfiguration mechanism can improve the prediction efficiency of fault diagnosis. The second one is to verify the consistency between the experimental results and the theoretical results.

4.2 Experiment Configuration

A multi-level centrifugal blower is used as the fault diagnosis device, as shown in Fig. 4. There are inner ring wear faults and outer ring wear faults on the rolling bearing shown in Fig. 5.

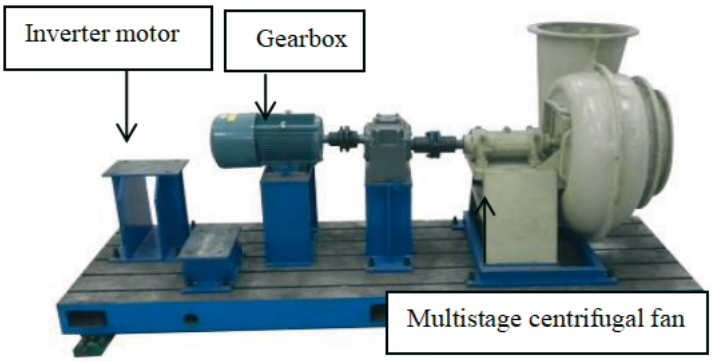

Fig. 4 Experimental platform of the multi-level centrifugal blower

Fig. 5 Gear and bearing faults detected in the gearbox

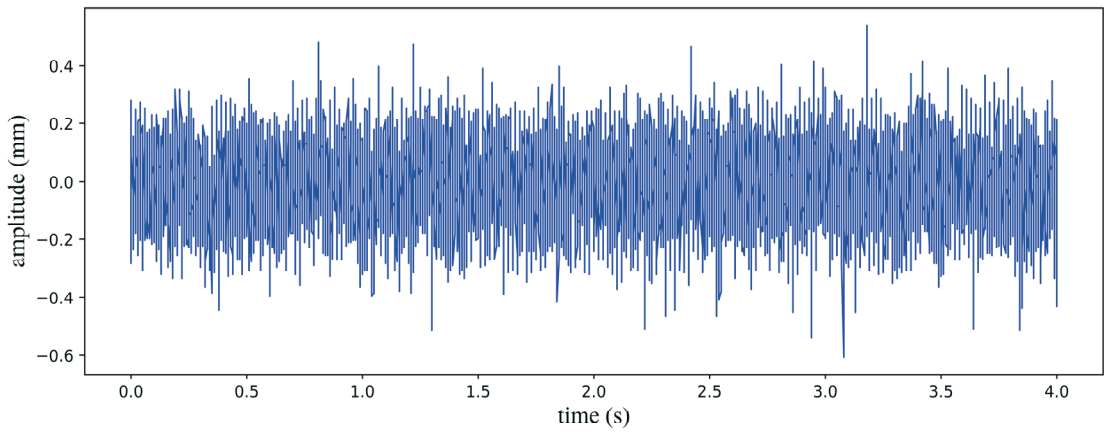

Fig. 6 Vibration waveform

Experimental platform-related parameters are as follows: the inverter motor rated voltage, current, and power are 380 V, 24.8 A, and 11 kW; The multistage centrifugal fan rated power is 11 kW, the maximum speed is 2970 r/min, and the blowing rate 8 m^3/min. Parameters related to the data collector are: acceleration 0.1~199.9 m/s^2, acquisition frequency 10 Hz~ 10 kHz, number of groups 1~100, and sampling points 512, 1024, 2048, and so on.

First, we can use the data acquisition software to collect the vibration signal, shown in Fig. 6. Then, the waveform index, impulsion index, tolerance index, peak index, and kurtosis index of the vibration signal are calculated, as shown in Table 6. The support vector machine (SVM) algorithm was used to train the predictive model.

Table 6 Definitions of five dimensionless parameters of the vibration signal

Dimensionless parameters	Theoretical calculation formula	Actual calculation formula
Waveform index	$S_f = \frac{\left[\int_{\Re} \lvert z\rvert^2 p(z)\mathrm{d}z\right]^{1/2}}{\left[\int_{\Re} \lvert z\rvert p(z)\mathrm{d}z\right]} = \frac{\sqrt{E(\lvert z\rvert^2)}}{E(\lvert z\rvert)}$	$S_f = \frac{\sqrt{\sum_{i=1}^{N} x_i^2 / N}}{\sum_{i=1}^{N} \lvert x_i\rvert / N}$
Impulse index	$I_f = \lim_{l\to\infty} \frac{\left[\int_{\Re} \lvert z\rvert^l p(z)\mathrm{d}z\right]^{1/l}}{\left[\int_{\Re} \lvert z\rvert p(z)\mathrm{d}z\right]} = \frac{\lim_{l\to\infty} \sqrt[l]{E(\lvert z\rvert^l)}}{E(\lvert z\rvert)}$	$I_f = \frac{\max(x_i)}{\sum_{i=1}^{N} \lvert x_i\rvert / N}$
Margin index	$CL_f = \lim_{l\to\infty} \frac{\left[\int_{\Re} \lvert z\rvert^l p(z)\mathrm{d}z\right]^{1/l}}{\left[\int_{\Re} \lvert z\rvert^{1/2} p(z)\mathrm{d}z\right]^2} = \frac{\lim_{l\to\infty} \sqrt[l]{E(\lvert z\rvert^l)}}{\left[E(\sqrt{\lvert z\rvert})\right]^2}$	$CL_f = \frac{\max(x_i)}{(\sum_{i=1}^{N} \lvert x_i\rvert / N)^2}$
Peak index	$C_f = \lim_{l\to\infty} \frac{\left[\int_{\Re} \lvert z\rvert^l p(z)\mathrm{d}z\right]^{1/l}}{\left[\int_{\Re} \lvert z\rvert^2 p(z)\mathrm{d}z\right]^{1/2}} = \frac{\lim_{l\to\infty} \sqrt[l]{E(\lvert z\rvert^l)}}{\sqrt{E(\lvert z\rvert^2)}}$	$C_f = \frac{\max(x_i)}{\sqrt{\sum_{i=1}^{N} x_i^2 / N}}$
Kurtosis index	$K_v = \frac{\int_{\Re} z^4 p(z)\mathrm{d}z}{\left[\int_{\Re} z^2 p(z)\mathrm{d}z\right]^2} = \frac{E(\lvert z\rvert^4)}{\left[E(\lvert z\rvert^2)\right]^2}$	$K_v = \frac{\sum_{i=1}^{N} x_i^4 / N}{\left(\sqrt{\sum_{i=1}^{N} x_i^2 / N}\right)^4}$

4.3 Analysis of the Experiment

4.3.1 Analysis of the Matthew effect prediction results

Figure 7 shows the consistency of the experimental results with the theoretical results.

As can be seen form Table 7 and Fig. 7, the prediction accuracy sharply increases with the increase in sample sequence length, which proves that the test set reconfiguration mechanism can improve the prediction accuracy effectively.

From Table 7, we can also note that when P_{11}=0.837 and the value corresponding to the length 50 is smaller than that of 45, the difference is 0.003. When P_{22}=0.769, the value

corresponding to the length 40 is smaller than that of 35, and the difference is 0.006. For the sample sequence with memorability, the experimental prediction accuracy increases less rapidly than that of the corresponding theoretical results. The cause of the difference in results is explained below.

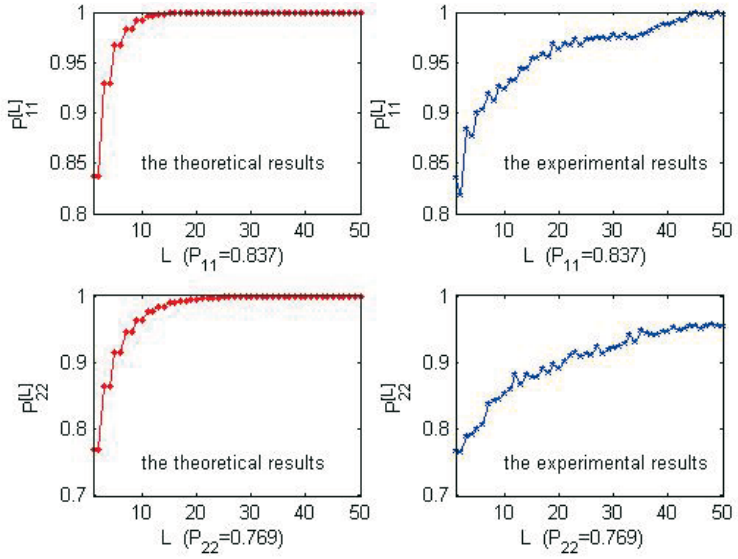

Fig. 7 Comparison between the experimental and theoretical results

Table 7 Comparison between the experimental and theoretical results

Sequence length	P_{11}=0.837		P_{22}=0.769	
	Experimental results	Theoretical results	Experimental results	Theoretical results
5	0.900	0.967	0.800	0.916
10	0.928	0.992	0.851	0.965
15	0.954	0.999	0.878	0.989
20	0.963	1.000	0.892	0.995
25	0.973	1.000	0.913	0.998
30	0.975	1.000	0.914	0.999
35	0.977	1.000	0.949	1.000
40	0.987	1.000	0.943	1.000
45	1.000	1.000	0.955	1.000
50	0.997	1.000	0.957	1.000

As can be seen in Fig. 8, the average prediction accuracy is 0.837. If the sample sequence length is 100, the prediction accuracy decreases/increases with the variation in sample numbers. Consequently, there is a difference between the experimental and theoretical results.

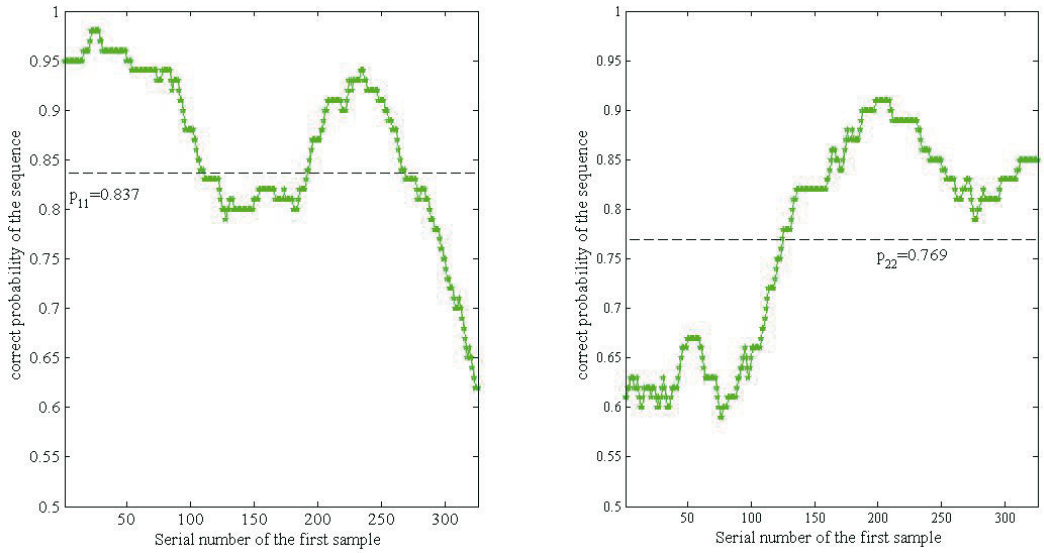

Fig. 8 Variation in the average prediction accuracy

4.3.2 Analysis of experimental results of delay minimization

Table 8 Experimental results 1

Fault type	Accuracy of SVM	Sequence length	Delay duration (unit: second)	The accuracy of our method
Normal	0.83	3	6	0.91
Gear tooth wear	0.68	13	26	0.91
A bearing without one ball	0.73	7	14	0.91
Bearing outer ring wear	0.76	5	10	0.91
Bearing inner ring wear	0.65	17	34	0.90

Table 9 Experimental results 2

Fault type	Accuracy of SVM	Sequence length	Delay duration (unit: second)	The accuracy of our method
Normal	0.83	5	10	0.95
Gear tooth wear	0.68	19	38	0.95
A bearing without one ball	0.73	11	22	0.95
Bearing outer ring wear	0.76	9	18	0.96
Bearing inner ring wear	0.65	29	58	0.95

In this experiment, in addition to the normal state, four fault states, i.e. gear tooth wear, lack of one ball in a bearing, bearing outer ring wear, and bearing inner ring wear were selected. It can be seen from Table 8 and Table 9 that the accuracy of bearing inner ring wear fault obtained by the support vector machine is only 0.65; on the other hand, the accuracy obtained

by using the method presented in this paper can reach 90% for the sequence length $L = 17$, and 95% for the sequence length $L = 29$, while the delay is 34 seconds and 58 seconds, respectively.

Table 10 Experimental results 3

Fault type	Accuracy of KNN	Sequence length	Delay duration (unit: second)	The accuracy of our method
Normal	0.81	3	6	0.90
Gear tooth wear	0.60	14	28	0.91
A bearing without one ball	0.69	8	16	0.90
Bearing outer ring wear	0.77	5	10	0.91
Bearing inner ring wear	0.61	19	38	0.90

AS can be seen from Table 8 and Table 10, the same effect can be achieved by replacing the SVM algorithm with the k-nearest neighbours (KNN) algorithm.

5. Conclusion

This paper presents a test set reconfiguration mechanism for classification problems of fault diagnosis. The classification mechanism of sample sequence to be classified with memory has the Matthew effect. Using the Matthew effect of accumulated advantage can improve the accuracy of fault classification. Using the delay minimization model, we can not only meet the requirement for a short-time delay but also get a high prediction accuracy.

Acknowledgment

This study was supported by the grants (No. 61473094, No.22078072, No. 61933013) from NSF of China.

REFERENCES

[1] Y. Jiang, S. Yin, O. Kaynak. Performance Supervised Plant-Wide Process Monitoring in Industry 4.0: A Roadmap.IEEE Open Journal of the Industrial Electronics Society, PP(99):1-1, 2020. https://doi.org/10.1109/OJIES.2020.3046044

[2] A. Niederlinski. A heuristic approach to the design of linear multivariable interacting control systems. Automatica J. IFAC, vol. 7, no. 6, pp. 691-701, 1971. https://doi.org/10.1016/0005-1098(71)90007-0

[3] P. M. Frank. Fault diagnosis in dynamics systems using analytical and knowledge-based redundancy: a survey and some new results. Automatica J. IFAC, vol. 26, no. 3, pp. 459-474, 1990. https://doi.org/10.1016/0005-1098(90)90018-D

[4] R. Beard. Failure accommodation in linear system through self-reorganization. Ph.D. issertation, MIT, Cambridge, MA, USA, 1971.

[5] E. Henley. Application of expert systems to fault diagnosis. In Proc. AICHE Annu. Meet., San Francisco, CA, USA 1984.

[6] M. C. Deng. Inoue A, Edahiro K. Fault Detection System Design for Actuator of a Thermal Process Using Operator Based Approach. Acta Automatica Sinica, vol. 36, no. 4, pp. 580-585, 2010. https://doi.org/10.1016/S1874-1029(09)60025-2

[7] S. H. You, Y. M. Cho, J. O. Hahn. Model-based fault detection and isolation in automotive yaw moment control system. International Journal of Automotive Technology, vol. 18, no. 3, pp. 405-416, 2017. https://doi.org/10.1007/s12239-017-0041-5

[8] D. Stavrou , D.G. Eliades, C. G. Panayiotou, et al. Fault detection for service mobile robots using model-based method. Autonomous Robots, vol. 40, no. 2, pp. 383-394, 2016. https://doi.org/10.1007/s10514-015-9475-7

[9] J. Choi, K. Yi, J. Suh, and B. Ko. Coordinated control of motor-driven power steering torque overlay and differential braking for emergency driving support. IEEE Trans. Vehicular Technology vol. 63, no. 2, pp. 566−579, 2014. https://doi.org/10.1109/TVT.2013.2279719

[10] H. Lee. Analysis of model-based sensor fault diagnosis with application to a motor-driven power steering system. Proc. Institution of Mechanical Engineers, Part D: J. Automobile Engineering vol. 225, no. 10, pp. 1317−1333, 2011. https://doi.org/10.1177/0954407011404506

[11] M. Oudghiri, M. Chadli, and E.l. Hajjaji. A Robust observer-based fault tolerant control for vehicle lateral dynamics. Int. J. Vehicle Design nol. 48, pp. 3-4, and pp. 173−189, 2008. https://doi.org/10.1504/IJVD.2008.022575

[12] J. Liu, Q. Li, W. Chen, et al. A discrete hidden Markov model fault diagnosis strategy based on K-means clustering dedicated to PEM fuel cell systems of tramways. International Journal of Hydrogen Energy, 2018. https://doi.org/10.1016/j.ijhydene.2018.04.163

[13] F. Bagheri, H. Khaloozaded, K. Abbaszadeh. Stator fault detection in induction machines by parameter estimation, using adaptive kalman filter. IEEE. vol. 3, no. 3-4, pp. 72-82, Jul. 2007. https://doi.org/10.1109/MED.2007.4433953

[14] L. L. Li, D. H. Zhou. Fast and robust fault diagnosis for a class of nonlinear systems: detectability analysis. comput. Chem. Eng., vol. 28, no. 12, pp. 2635-2646, Nov. 2004. https://doi.org/10.1016/j.compchemeng.2004.07.023

[15] C. Li, W. Yan, C. Jing, et al. Fault Diagnosis in a Gyroscope-Based Six-Axis Accelerometer. Transactions of FAMENA, vol. 42, no. 3, pp. 103-114, 2018. https://doi.org/10.21278/TOF.42307

[16] S. Ding, S. Yin, K. Peng, H. Hao, and B. Shen. A novel scheme for key performance indicator prediction and diagnosis with application to an industrial hot strip mill. IEEE Trans. Ind. Informat., nol. 9, no. 4, pp. 2239-2247, 2013. https://doi.org/10.1109/TII.2012.2214394

[17] R. Vitale, O. E. D. Noord, A. Ferrer. A kernel-based approach for fault diagnosis in batch processes. Journal of Chemometrics. pp. S697-S707, 2014. https://doi.org/10.1002/cem.2629

[18] L. J. Luo, S. Y. Bao, J. F. Mao; Z. Y. Ding. Industrial Process Monitoring Based on Knowledge-Data Integrated Sparse Model and Two-Level Deviation Magnitude Plots. Industrial & EngineeringChemistry Research, vol. 57, no. 2, pp. 611-622, 2018. https://doi.org/10.1021/acs.iecr.7b02150

[19] X. Wang, J. Ren, S. Liu. Distribution Adaptation and Manifold Alignment for Complex Processes Fault Diagnosis. Knowledge-Based Systems, 2018. https://doi.org/10.1016/j.knosys.2018.05.023

[20] Z. Gao, C. Cecati. and S. X. Ding. A survey of fault diagnosis and fault-tolerant techniques − Part II, fault diagnosis with knowledge-based and hybrid/active approaches. IEEE Trans. Industrial Electronics vol. 62, no. 6, pp. 3768-3774, 2015. https://doi.org/10.1109/TIE.2015.2417501

[21] J. O. Estima, A. J. M. Cardoso. A New Algorithm for Real-Time Multiple Open-Circuit Fault Diagnosis in Voltage-Fed PWM Motor Drives by the Reference Current Errors. IEEE Transactions on Industrial Electronics, vol. 60, no. 8, pp. 3496-3505, 2013. https://doi.org/10.1109/TIE.2012.2188877

[22] P. Samara, G. Fouskitakis, J. Sakellariou and S. Fassois. A statistical method for the detection of sensor abrupt faults in aircraft control systems. IEEE Trans. Control Syst. Technol., vol. 16, no. 4, pp. 789-798, 2008. https://doi.org/10.1109/TCST.2007.903109

[23] L. Wen, X. Li, L. Gao, et al. A New Convolutional Neural Network-Based Data-Driven Fault Diagnosis Method[J]. IEEE Transactions on Industrial Electronics. vol. 65, no. 7, pp. 5990-5998, 2018. https://doi.org/10.1109/TIE.2017.2774777

[24] Z. Zhou, C. Wen, C. Yang. Fault Isolation Based on k-Nearest Neighbor Rule for Industrial Processes. IEEE Transactions on Industrial Electronics, vol. 63, no. 4, pp. 2578-2586, 2016. https://doi.org/10.1109/TIE.2016.2520898

[25] Q. Zhang, D. Zhou, X. Zeng. HeartID: A Multiresolution Convolutional Neural Network for ECG-based Biometric Human Identification in Smart Health Applications. IEEE Access, pp(99):1-1, 2017. https://doi.org/10.1109/ACCESS.2017.2707460

[26] M. Zhao, M. Kang, B. Tang, et al. Deep Residual Networks With Dynamically Weighted Wavelet Coefficients for Fault Diagnosis of Planetary Gearboxes. IEEE Transactions on Industrial Electronics, vol. 65, no. 5, pp. 4290-4300, 2018. https://doi.org/10.1109/TIE.2017.2762639

[27] S. Li, H. Cao, Y. Yang. Data-driven simultaneous fault diagnosis for solid oxide fuel cell system using multi-label pattern identification. Journal of Power Sources, vol. 378, 2018. https://doi.org/10.1016/j.jpowsour.2018.01.015

[28] M. Khazaee, H. Ahmadi, M. Omid, et al. Feature-level fusion based on wavelet transform and artificial neural network for fault diagnosis of planetary gearbox using acoustic and vibration signals. Insight:Non-Destructive Testing and Condition Monitoring, vol. 55, no. 6, pp. 32-329, 2013. https://doi.org/10.1784/insi.2012.55.6.323

[29] Y. Jiang, S. Yin, O. Kaynak. Optimized Design of Parity Relation-Based Residual Generator for Fault Detection: Data-Driven Approaches. IEEE Transactions on Industrial Informatics, vol. 17, no. 2, pp. 1449-1458, 2021. https://doi.org/10.1109/TII.2020.2987840

[30] F. Alcala, S. J. Qin. Reconstruction-based contribution for process monitoring. Ind. Eng. Chem. Res, vol. 49, no. 17, pp.7849-7857, Mar. 2010. https://doi.org/10.1021/ie9018947

[31] L. Lardon, A. Punal, J. P. Steyer. On-line diagnosis and uncertainty management using evidence theory-experimental illustration to anaerobic digestion processes. J. Process Control, vol. 14, no. 7, pp. 747-763, 2004. https://doi.org/10.1016/j.jprocont.2003.12.007

[32] Castro, A. Ranson, J. Matheus, et al. Fault detection and identification in chemical processes using multivariable statistical techniques and SVM for classification. In Proc of Isa Monterrey 2002(English), vol. 433, pp.165-175, 2002.

[33] H. Wu, J. Zhao. Deep convolutional neural network model based chemical process fault diagnosis. Computers & Chemical Engineering, 2018. https://doi.org/10.1016/j.compchemeng.2018.04.009

[34] Deng, and Wang. A Novel Evidence Conflict Measurement for Multi-Sensor Data Fusion Based on the Evidence Distance and Evidence Angle. Sensors ,vol. 20, no. 2, pp.381, 2020. https://doi.org/10.3390/s20020381

[35] Q. Basir, X. Yuan. Engine fault diagnosis based on multi-sensor information fusion using Dempster-Shafer evidence theory. Information Fusion, vol. 8, no.4, pp. 379-386, 2007. https://doi.org/10.1016/j.inffus.2005.07.003

[36] J. Ni, C. Zhang, S. X. Yang. An Adaptive Approach Based on KPCA and SVM for Real-Time Fault Diagnosis of HVCBs. IEEE Transactions on Power Delivery, vol. 26, no. 3, pp. 1960-1971, 2011. https://doi.org/10.1109/TPWRD.2011.2136441

[37] M. M. Manjurul, J. M. Kim. Reliable Multiple Combined Fault Diagnosis of Bearings Using Heterogeneous Feature Models and Multiclass Support Vector Machines. Reliability Engineering & System Safety, 2018. https://doi.org/10.1016/j.ress.2018.02.012

[38] Y. Xue, L. Zhang, B. Wang, et al. Nonlinear feature selection using Gaussian kernel SVM-RFE for fault diagnosis[J]. Applied Intelligence, pp. 1-26, 2018. https://doi.org/10.1007/s10489-018-1140-3

[39] S. Longqiu, Z. Qinghua, L. Gaowei, et al. An Immune Detector-Based Method for the Diagnosis of Compound Faults in a Petrochemical Plant. Transactions of FAMENA, vol. 46, no. 3, pp. 1-12, 2022. https://doi.org/10.21278/TOF.463033721

[40] S. Naiquan, Z. Zhijie, Z. Qinghua, et al. Fault Feature Extraction of Bearings for the Petrochemical Industry and Diagnosis Based on High-Value Dimensionless Features. Transactions of FAMENA, vol. 46, no. 4, pp. 31-44, 2022. https://doi.org/10.21278/TOF.464036521

Submitted: 16.3.2022

Accepted: 15.01.2023

Dr. Shihua Wang*
School of Science, Guangdong University of Petrochemical Technology, Maoming 525000, China
Prof. Shaolin Hu
Prof. Qinghua Zhang
School of Automation, Guangdong University of Petrochemical Technology, Maoming 525000, China
*Corresponding author:
wangshihuaxx@163.com